

This article was presented at the LII Scientific and Educational Conference of ITMO University, January 31 – February 03, 2023, St. Petersburg, Russia

Oxygen Saturation Monitor Model Design for Freediving Implementation

K.R. Razzhivina*, A.V. Kamarchuk, D.S. Shiryayev

Institute of Advanced Data Transfer Systems, ITMO University, Kronverkskiy pr., 49, lit. A, St. Petersburg, 197101, Russia

Article history

Received March 06, 2023
Received in revised form
March 26, 2023
Accepted March 28, 2023
Available online March 31, 2023

Abstract

This paper describes the operation model of reflectance oxygen saturation monitor for freediving implementation and its dependence on distance and interposing media between the monitor and human skin. The model includes two LEDs with peak radiation wavelengths 660 nm and 940 nm and two photodiodes with peak sensitivity at 940 nm, interposing medium layer with air, water or silica glass parameters and seven skin layers. The modeling is executed by Monte-Carlo method for the cases of air, glass and water as interposing medium and its various width in range from 2 mm to 8 mm which is chosen due to the planned case construction. The energy fluxes ratio dependence on distance between the photodiodes and skin is evaluated and analyzed.

Keywords: Pulse oximetry; Freediving; Oxygen saturation; Photoplethysmography; Optical properties of skin

1. INTRODUCTION

Pulse oximetry as a noninvasive method for monitoring oxygen saturation has become widely known in medicine and sport. However, there are still several limitations in oxygen saturation monitors determining the usage such as certain monitor locality and inconvenience of attachment to human body for measurements with transmittance probe usage, monitor inability to measure saturation in motion, and low accuracy for reflectance probes [1]. These factors tend to decline the oxygen saturation monitors applicability in sport, particularly freediving. For freedivers not using any underwater breathing equipment it is inevitable to observe the heart rate and oxygen saturation during the training which may prevent the blackout or psychomotor retardation [2]. Therefore, the data transfer to trainer's personal computer is also required to modify the training process and make it more effective. There is a challenge in freediving to obtain an oxygen saturation monitor system which combines all the essential characteristics mentioned before. The designed oxygen saturation monitor model is presented in this paper to achieve the successful monitor system development.

Freediving implementation requires the maintenance of athlete mobility, on this account the reflectance probe was chosen. According to works [3–5] the accuracy of reflectance oxygen saturation monitor depends on the distance between the photodiodes and LEDs; therefore, the optimum distance was chosen — 6 mm between each photodiode and corresponding LED.

However, there are no works considering water as an interposing medium. Due to the continuous underwater usage of monitor it is vital to calculate the impact of water environment on the optical parameters of the monitor which is not presented in nowadays studies. Most models presented in works, for example [6,7], are connected to terrestrial applications and not appropriate for the freediving case. As stated earlier, there is a need to use the underwater operating monitor that can track the parameters during the training in spite of aquatic medium impact. Consequently, the reflectance oxygen saturation monitor model with study of water optical properties impact is one of particular interest for freediving application.

Hence, the goal of this work is to calculate the effect of interposing media such as water and glass on the oxygen saturation monitor behavior. The oxygen saturation

* Corresponding author: K.R. Razzhivina, e-mail: k.razzhivina@niuitmo.ru

Table 1. Optical properties of skin.

Skin layer	Saturation level	Wavelength 660 nm		Wavelength 940 nm	
		μ_a, mm^{-1}	μ_s, mm^{-1}	μ_a, mm^{-1}	μ_s, mm^{-1}
Stratum corneum	-	0.060	100	0.025	100
Living epidermis	-	0.075	45	0.075	60
Papillary dermis	-	0.016	30	0.120	30
Upper blood net dermis	70%	0.104	35	0.071	35
	100%	0.020	35	0.080	35
Dermis	-	0.010	25	0.150	25
	70%	0.104	30	0.071	35
Deep blood net dermis	100%	0.020	30	0.080	35
	-	0.010	5	0.140	15

monitor model including the 7-layered skin model, the location of LEDs and photodiodes, and interposing medium layer was developed and analyzed to reach the goal.

2. METHODS

For the oxygen saturation monitor two LEDs are selected with peak radiation wavelengths of 660 nm and 940 nm, which are conditioned by absorption spectra of hemoglobin. To ensure the same energy fluxes radiated from LEDs and to provide the components commercial availability different dimensional specifications of infrared and red sources were chosen. Thus, the size of infrared LED was chosen to be $3.5 \times 2.8 \times 0.8$ mm and red LED dimensions were $1.6 \times 0.8 \times 0.8$ mm. For each LED total energy flux is 100 mW and viewing angle is 120° .

According to the LEDs parameters and skin's high absorbance in infrared wavelength range, silicon photodiode with peak sensitivity at the wavelength 940 nm is chosen. As the values have to be precise, the sensitive surface area of the photodiode must be the largest available for the presented application limited only by packaging size. The market research shows that one of the most optimal options is 7.5 mm^2 which is used in presented model. The relative spectral sensitivity of the photodiode with the chosen parameters is 1.0 at 940 nm and 0.65 at 660 nm.

As there is a need to ensure the optimal mobility of the athlete, the oxygen saturation monitor design is based on reflectance-mode photoplethysmography which implied the placement of photodiodes and LEDs on the same side against the biological tissue.

To consider skin optical properties the 7-layered model was chosen which included stratum corneum (skin surface), living epidermis, papillary dermis, upper blood net dermis, dermis, deep blood net dermis and subcutaneous fat [8]. The choice of such model was conditioned by the necessity of blood nets differentiation and the accuracy of determining the impact of absorption and scattering coefficients [9,10]. Consequently, absorption coefficient μ_a and scattering

coefficient μ_s , refractive indices and anisotropy [11] of different skin layers on the wavelengths of 660 nm and 940 nm were estimated for Caucasian skin type [12]. Absorption and scattering coefficients of blood net layers were calculated according to work [13]. Table 1 provides the chosen coefficients.

The absorption and scattering coefficients of water were estimated using the works [14–16] according to the parameters of water in diving pools; chosen coefficients are shown in Table 2. The thickness of water layer was varied between 1 and 4 mm due to possible construction of oxygen saturation monitor case to provide the best option for the further case design. Silica glass was chosen as a part of package and modeled as one of the layers with thickness also varied from 1 to 4 mm, which is limited due to the need for a tight fit of the monitor on human body. Different combinations of water and glass thickness are presented in this work to describe the impact of different optical properties on the light propagation and to provide the qualitative analysis for further development.

The model of interaction between radiation of the oxygen saturation monitor and skin layers, glass and water were calculated using the Monte Carlo method of ray tracing. The absorption was described with the Lambert-Beer law:

$$I(z) = I_0 \exp(-\mu_a z), \quad (1)$$

where $I(z)$ is the light intensity dependence on distance z , I_0 is the initial intensity. For the scattering formulation the Henyey-Greenstein formula

$$p(\theta) = \frac{(1-g)^2}{(1+g^2-2g \cos \theta)^{3/2}}, \quad (2)$$

Table 2. Optical properties of water.

Coefficients	Wavelength 660 nm	Wavelength 940 nm
μ_a, m^{-1}	0.380	10.0
μ_s, m^{-1}	7	2

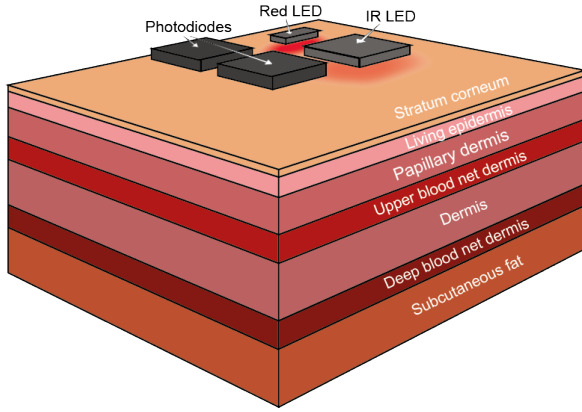


Fig. 1. Model general form.

where $p(\theta)$ is photon scattering probability function of the angle θ , g is the anisotropy factor, was applied as the most compliant with scattering in biological tissues [17]. To estimate the probability distribution to reach the certain distance in scattering media (skin) the following expression is also used:

$$P(x) = \exp(-\mu_s x), \quad (3)$$

where $P(x)$ is photon scattering probability function of the distance x .

Three different model cases were considered: (1) interaction with skin layers and air, (2) skin layers, glass and air, (3) skin layer, glass and water. The model general form is presented in Fig. 1.

To consider the results on whole photosensitive surface the value of energy flux is calculated with equation:

$$\Phi = \int I dS, \quad (4)$$

where Φ is the value of total energy flux at the photodiode surface in Watts, I is the energy flux density in W/m^2 , S is the photodiode surface area in m^2 .

To calculate the oxygen saturation the following formula is used:

$$SpO_2 = A - B \frac{(AC/DC)_{red}}{(AC/DC)_{infrared}}, \quad (5)$$

where SpO_2 is oxygen saturation, A and B are constants defined during the monitor calibration, AC and DC are alternating and direct currents, respectively, for red and infrared LEDs fluxes. Consequently, to estimate the saturation value it is necessary to calculate the ratio of normalized red and infrared fluxes; it is the final step of this paper.

3. RESULTS AND DISCUSSION

The calculation of interaction between radiation of the oxygen saturation monitor and skin layers showed that there is enough resulting power on the photodiode to induce the light current and differentiate the cases of low and high saturation. The obtained values are presented in Table 3 for different types of media between photodiodes and skin layers in width range from 2 mm to 8 mm.

The obtained values were compared for critical oxygen saturation values according to technical requirements for the oxygen saturation monitor: minimum at 70% and maximum at 100%. The differences in light flux on the photodiode surface for maximum and minimum value of saturation in dependence on distance between photodiodes and skin layers is depicted in Fig. 2. As a general trend, total flux declines with the distance increase which is connected

Table 3. The values of total flux on photodiode surface in dependence of material's width between photodiode and skin layers.

Width of material between photodiode and skin layers	Infrared light flux (μW),		Red light flux (μW),	
	$SpO_2 = 70\%$	$SpO_2 = 100\%$	$SpO_2 = 70\%$	$SpO_2 = 100\%$
2 mm air	483.2	486.1	733.5	781.3
1 mm glass, 1 mm water	805.4	793.4	1283.2	1368.9
3 mm air	388.3	393.7	586.8	633.9
1 mm glass, 2 mm water	667.3	664.3	1181.2	1254.3
2 mm glass, 1 mm water	819.7	825.4	1401.1	1502.6
4 mm air	292.0	320.7	324.1	484.7
2 mm glass, 2 mm water	630.1	627.2	1062.6	1132.3
5 mm air	264.0	259.5	354.6	377.5
1 mm glass, 4 mm water	508.4	502.2	833.9	887.0
4 mm glass, 1 mm water	782.3	628.3	1206.1	1121.4
6 mm air	188.1	186.9	248.3	268.5
2 mm glass, 4 mm water	502.8	505.2	777.7	831.9
4 mm glass, 2 mm water	646.0	643.8	950.5	1021.3
8 mm air	158.5	155.5	119.6	122.7
4 mm glass, 4 mm water	487.9	487.3	816.2	873.2

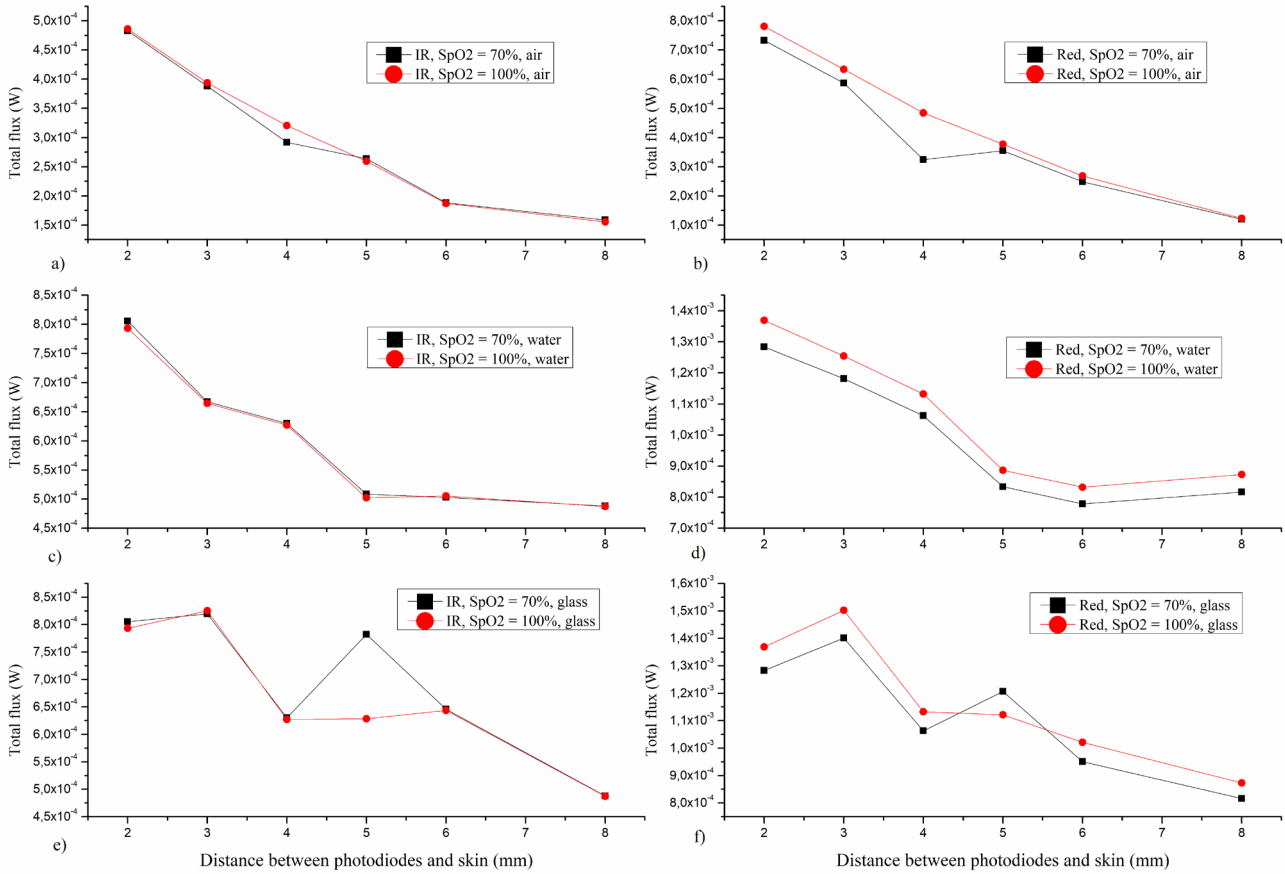


Fig. 2. The differences in flux on the photodiode surface for maximum and minimum value of saturation in dependence of distance between photodiodes and skin layers: a) case of infrared LED radiation and air between photodiode and skin; b) case of red LED radiation and air; c) case of infrared LED radiation and larger water layer width; d) case of red LED radiation and larger water layer width; e) case of infrared LED radiation and larger glass layer width; f) case of red LED radiation and larger glass layer width.

to the partial absorption of LEDs radiation by interposing media. The differences between the flux in case of minimum and maximum saturation values are visible for red LED radiation and almost identical to each other for infrared LED radiation. However, there are several fluctuating points: for example, at 4 mm air width or 4 mm of glass and 1 mm of water, which show the greatest distinction between 70% and 100% oxygen saturation. The fluctuation is explained with the interposing media scattering and reflection; light propagation properties which are considered in model such as photon multiple scattering angle are slightly changed due to the distance alteration. The interposing medium also impacts the total flux value: it is increased in case of water and glass due to their higher reflection coefficients compared to ones of air.

It is important to estimate the ratio of red and infrared fluxes for further saturation calculations. Thus, red and infrared fluxes ratio dependence of distance between the photodiodes and skin layer at critical saturation levels is shown in Fig. 3. The ratio value becomes higher when interposing medium includes glass and water compared to only air. That effect is reached by chromatic dispersion in glass and water, and, consequently, more

differences between the light propagation in case of red and infrared LED radiation which means oxygen saturation monitor works more effectively. Taking into consideration silica glass and water optical properties silica glass effects the light propagation so that the red and infrared fluxes ratio is 20% higher than in the same case with water. The contrast between the ratios for minimum and maximum saturation values is steady for all the distances modeled, and it is easy to distinguish which is vital for further signal processing.

4. CONCLUSIONS

The reflectance oxygen saturation monitor model was designed and calculated to identify the monitor system operation efficiency. The modeling was executed by Monte Carlo method considering silica glass and water as interposing media between the photodiodes and skin layers. The obtained flux values showed that glass and water optical properties provide the optimal red and infrared fluxes ratio for further signal processing on analog-digital converter and saturation value calculations. Presented results express the stability in flux differences for minimum and

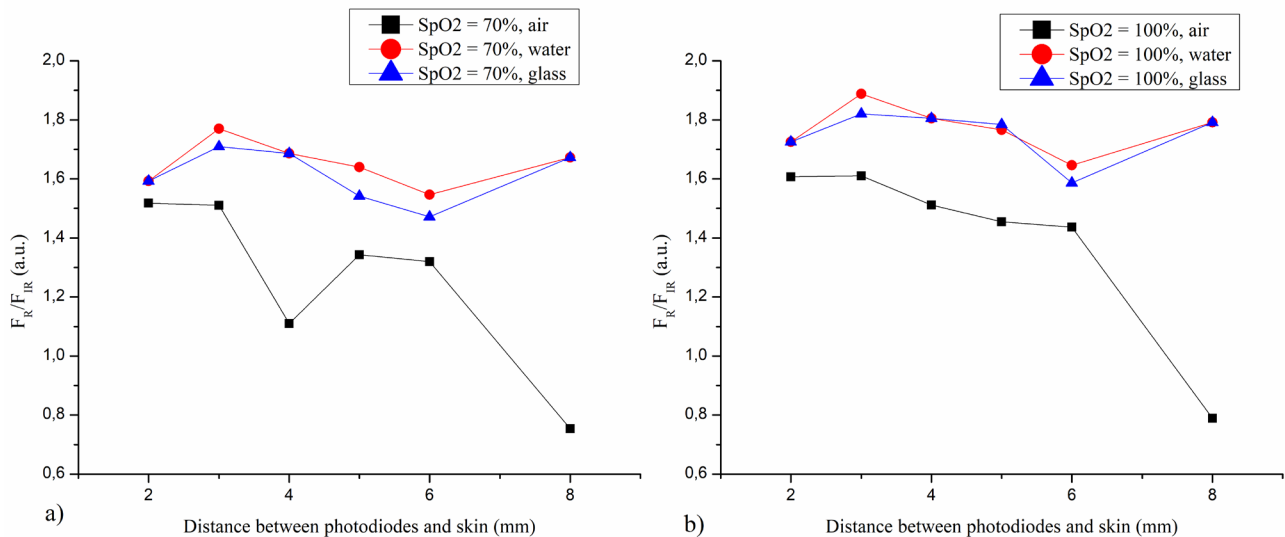


Fig. 3. Red and infrared fluxes ratio dependence on distance between the photodiodes and skin layer at: (a) minimum saturation level; (b) maximum saturation level.

maximum saturation values; however, the highest flux values are reached in case of 2 mm glass layer and 1 mm water layer as interposing media which is going to be used for the oxygen saturation monitor construction due to the necessary signal processing in electrical circuit and signal attenuation.

REFERENCES

- [1] T. Tamura, Y. Maeda, M. Sekine, M. Yoshida, *Wearable photoplethysmographic sensors—past and present*, *Electronics*, 2014, vol. 3, no. 2, pp. 282–302.
- [2] J. Chmura, A. Kawczynski, M. Medras, P. Jozkow, B. Morawiec, *The impact of freediving on psychomotor performance and blood catecholamine concentration*, *Undersea and Hyperbaric Medicine*, 2014, vol. 41, no. 2, pp. 111–117.
- [3] J.G. Webster (ed.), *Design of pulse oximeters*, CRC Press, 1997.
- [4] Y. Mendelson, B.D. Ochs, *Noninvasive pulse oximetry utilizing skin reflectance photoplethysmography*, *IEEE Transactions on Biomedical Engineering*, 1988, vol. 35, no. 10, pp. 798–805.
- [5] G. Di, X. Tang, W. Liu, *A reflectance pulse oximeter design using the MSP430F149*, in: 2007 IEEE/ICME International Conference on Complex Medical Engineering, IEEE, 2007, pp. 1081–1084.
- [6] M. Mehrabi, S. Setayeshi, M.G. Maragheh, S.H. Ardehali, H. Arabalibeik, *Design of a new reflectance pulse oximeter by obtaining the optimal source-detector space*, *Optik*, 2018, vol. 168, pp. 34–45.
- [7] I.B. Isupov, R.S. Zatrudina, *Electronic module for photoplethysmography and pulse oximetry*, *Natural Systems and Resources*, 2018, vol. 8 no. 3, pp. 15–21.
- [8] I.V. Meglinski, S.J. Matcher, *Quantitative assessment of skin layers absorption and skin reflectance spectra simulation in the visible and near-infrared spectral regions*, *Physiological Measurement*, 2002, vol. 23, no. 4, art. no. 741.
- [9] C. Donner, H.W. Jensen, *A Spectral BSSRDF for Shading Human Skin*, in: Proceedings of the 17th Eurographics Conference on Rendering Techniques (EGSR '06), Eurographics Association, Goslar, DEU, 2006, pp. 409–418.
- [10] L.O. Svaasand, L.T. Norvang, E.J. Fiskerstrand, E.K.S. Stopps, M.W. Berns, J.S. Nelson, *Tissue parameters determining the visual appearance of normal skin and port-wine stains*, *Lasers in Medical Science*, 1995, vol. 10, pp. 55–65.
- [11] T. Lister, P.A. Wright, P.H. Chappell, *Optical properties of human skin*, *Journal of Biomedical Optics*, 2012, vol. 17, no. 9, art. no. 090901.
- [12] H. Ding, J.Q. Lu, W.A. Wooden, P.J. Kragel, X.H. Hu, *Refractive indices of human skin tissues at eight wavelengths and estimated dispersion relations between 300 and 1600 nm*, *Physics in Medicine & Biology*, 2006, vol. 51, no. 6, art. no. 1479.
- [13] H. Liu, B. Chance, A.H. Hielscher, S.L. Jacques, F.K. Tittel, *Influence of blood vessels on the measurement of hemoglobin oxygenation as determined by time-resolved reflectance spectroscopy*, *Medical Physics*, 1995, vol. 22, no. 8, pp. 1209–1217.
- [14] H. Buiteveld, J.H.M. Hakvoort, M. Donze, *Optical properties of pure water*, *Proceedings of SPIE*, 1994, vol. 2258, pp. 174–183.
- [15] R.M. Pope, E.S. Fry, *Absorption spectrum (380–700 nm) of pure water. II. Integrating cavity measurements*, *Applied Optics*, 1997, vol. 36, no. 33, pp. 8710–8723.
- [16] S.J. Matcher, M. Cope, D.T. Delpy, *Use of the water absorption spectrum to quantify tissue chromophore concentration changes in near-infrared spectroscopy*, *Physics in Medicine & Biology*, 1994, vol. 39, no. 1, art. no. 177.
- [17] M.H. Niemz, *Laser-tissue interactions*, Springer-Verlag, Berlin, Heidelberg, 2007.

УДК 535.8

Разработка модели пульсоксиметрического датчика для применения во фридайвинге

К.Р. Разживина, А.В. Камарчук, Д.С. Ширяев

Институт перспективных систем передачи данных, Университет ИТМО, Кронверкский пр., 49, лит. А, Санкт-Петербург,
197101, Россия

Аннотация. В данной работе описана модель работы рефракционного пульсоксиметрического датчика для применения его во фридайвинге и зависимость модели работы от расстояния и среды между датчиком и кожей человека. Модель включает в себя два светодиода с пиковыми длинами волн излучения 660 нм и 940 нм и два фотодиода с пиковой чувствительностью на длине волны 940 нм, слой среды между датчиком и кожей с заданными параметрами воздуха, воды или кварцевого стекла и 7 слоев кожи. Моделирование проводилось методом Монте-Карло для воздуха, воды и стекла в качестве среды между датчиком и кожей и различными её толщинами в диапазоне от 2 мм до 8 мм, что обусловлено особенностями планируемого корпуса. Была определена и проанализирована зависимость отношения световых потоков от расстояния между фотодиодами и кожей.

Ключевые слова: пульсоксиметрия; фридайвинг; насыщение кислородом; фотоплетизмография; оптические свойства кожи